Nanoscale

Accepted Manuscript

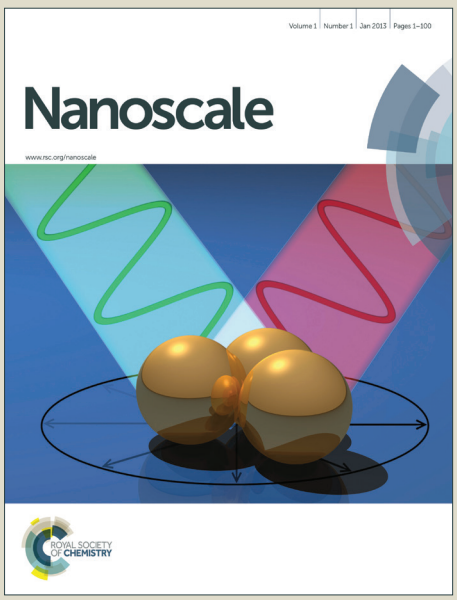

ROYAL SOCIETY OF CHEMISTRY

www.rsc.org/nanoscale

Nanoscale

ARTICLE

Stabilization of Ultrafine Metal Nanocatalysts on Thin Carbon Sheets †

Received 00th January 20xx,
Accepted 00th January 20xx

DOI: 10.1039/x0xx00000x

www.rsc.org/

Xiaofang Liu,[*a,b] Xinrui Cui,[a] Yiding Liu,[b] and Yadong Yin[*b]

A novel strategy was proposed to anchor ultrafine metal nanoparticles (NPs) on thin carbon sheets for highly stable and efficient heterogeneous catalysts. In this facile approach, a dense monolayer of ultrafine AuNPs was sandwiched between a silica core and a resin shell, followed by carbonization of the shell at a high temperature and then selective removal of the silica core. The shrinkage of the shells during carbonization facilitates partial embedment of the AuNPs in the carbon shell surface and enables superior stability against particle sintering during high temperature/mechanical post-treatments and catalytic reactions. It was also found that diffusion of reactants to the surface of AuNPs could be maximized by reducing the thickness of the hollow shells or simply by cracking the shells into thin carbon sheets, both significantly benefiting the high catalytic efficiency. The advantages of this ultra stable architecture together with the densely dispersed catalytic sites were demonstrated by the high stability and superior catalytic activity in reducing hydrophilic 4-nitrophenol and hydrophobic nitrobenzene.

Introduction

Heterogeneous catalysts based on metal nanoparticle (NP) have attracted tremendous research interest in recent decades due to their promising applications in catalyzing a variety of chemical reactions and the advantages of being easily recoverable and reusable.[1-6] Generally, metal NPs are loaded on some kind of supports (like carbon, SiO_2 etc.) as the catalyst. The mass/volumetric activities of the catalyst could be significantly improved by reducing the particle size of the catalysts and increasing their distribution density.[7] However, small-sized metal NPs tend to agglomerate into large ones during reactions especially at high temperatures, and thus cause activity decay.[8] Therefore, how to improve the dispersion stability of catalyst NPs on the support is a critical concern in designing and synthesizing high-performance heterogeneous catalysts.

Yolk-shell structure has been intensively investigated recently for dispersing catalyst NPs by encapsulating the particles in the hollow shells. "Yolk" could be various noble metal NPs and the "shell" could be many mesoporous materials. During the catalytic process, the catalyst NPs can be effectively confined in the nanoscale reactors without leakage and aggregation. Until now, many yolk-shell heterogeneous catalysts, such as Au@ZrO_2,[9] Au@TiO_2,[10] Au@polymer,[11] Au@CeO_2,[12] Pt@CoO,[13] and Pd@SiO_2[14] have been synthesized and showed stable catalytic activity after several times of recycling. However, such structures still have drawbacks. Firstly, as the synthesis of such structures usually involves sequential coating processes, the size of the catalyst NPs is usually larger than 10 nm, while extension to even smaller nanoparticles, which are more catalytically relevant, often faces problems of aggregation. Such a challenge leads to a relatively low mass utilization of the metal catalysts. Secondly, each hollow sphere contains only one active particle, which leads to a relatively low distribution density of the catalytic NPs. Thirdly, the connection between catalytic NPs and the support is loose in the yolk-shell structure, that makes insufficient electronic contact between active NPs and support, which is a critical parameter for electrochemical catalysis applications, such as fuel cells.[15] To disperse multiple small NPs in one yolk-shell unit, efforts have been made to load many ultrafine NPs into mesoporous shells, or to link multiple metal NPs to the supports through molecular connections.[11, 16-18] However, the linkages between the pre-formed supports and post-injected catalyst NPs were usually weak and the movement and agglomeration of catalyst NPs could not be completely avoided. In addition to addressing the challenges for stabilization of ultrafine catalyst NPs while maintaining high activity, further development of such advanced heterogeneous catalysts is expected to sustain intensive thermal, mechanical and/or corrosion impacts, given that many practical applications involve high temperature, vigorous stirring or harsh chemicals.

In this work, we report a novel strategy towards the design of advanced heterogeneous catalysts by stabilizing densely dispersed ultrafine AuNPs to the surface of thin carbon sheets (denoted as Au/C thin sheets). Through a sol-gel based templating method, a dense monolayer of AuNPs (less than 5 nm) were embedded in the inner walls of hollow carbon spheres, which were then cracked to fully expose the AuNP catalysts to the reactants. For each individual AuNP, the carbon support tightly wraps a part of the particle and leaves the other part exposing to the reactants for catalysis reactions. Detachment and agglomeration of the AuNPs, thus can be effectively prevented, even after being treated at a high temperature (800 ^{o}C) or vigorous mechanical grinding. The

[a] School of Materials Science and Engineering, Beihang University, Beijing 100191, China. E-mail: liuxf05@buaa.edu.cn
[b] Department of Chemistry, University of California, Riverside, CA 92521, USA. E-mail: yadongy@ucr.edu

† Electronic supplementary information (ESI) available: Size distribution and UV-vis absorption spectrum of the as-prepared AuNPs, N_2 adsorption–desorption isotherm of Au/C hollow spheres, UV-vis spectral change of reduction of nitrobenzene catalyzed by Au/C thin sheets. See DOI: 10.1039/c3nr01977b

templating/etching process involved in the synthesis also renders water dispersity to the inherently hydrophobic carbon shells. As a result, with unhindered diffusion and high stability, the Au/C thin sheets exhibit excellent catalytic efficiency and recyclability in the reduction of both hydrophilic nitrophenol and hydrophobic nitrobenzene. Compared to oxide supports such as SiO_2 and TiO_2, the carbon support has additional benefits for the applications in harsh environment due to its excellent chemical inertness.

Experimental

Chemicals

Ethanol (denatured), 2-propanol (99.9%), ammonium hydroxide aqueous solution (28%), 3-aminopropyl-triethoxysilane (APTES, 99%), and formaldehyde (37% solution) were obtained from Fisher Scientific. Tetraethyl orthosilicate (TEOS, 98%), hydrogen tetrachloroaurate (III) trihydrate ($HAuCl_4 \cdot 3H_2O$, 99.9+%), sodium citrate tribasic dihydrate (99%), resorcinol, cetyltrimethylammonium bromide (CTAB, 98%), sodium hydroxide (NaOH) and sodium borohydride ($NaBH_4$, 99%) were obtained from Sigma-Aldrich. All chemicals were directly used as received without further treatment.

Synthesis of SiO_2 templates

SiO_2 spheres with diameter of ~450 nm were synthesized through a modified Stöber method.[19, 20] In a typical synthesis, 1 mL of TEOS was injected into a mixture of 4 mL of deionized water, 1 mL of $NH_3 \cdot H_2O$ and 20 mL of 2-propanol at room temperature under magnetic stirring. After reacting for 4 h, the colloidal spheres were collected by centrifugation and washed with ethanol for three times.

Synthesis of Au nanoparticles

Gold nanoparticles were prepared according to the standard sodium citrate reduction method. Briefly, 0.5 ml of $HAuCl_4$ aqueous solution (10 mM) and 0.5 ml of trisodium citrate aqueous solution (10 mM) were added to 18.5 ml of milli Q water under vigorously stirring, followed by injection of 0.5 ml of $NaBH_4$ aqueous solution (0.1 M) which initiated the reduction of $HAuCl_4$. The solution was stirred for 5 min and aged for at least 3 h, yielding a stable, red dispersion of AuNPs with an average diameter below 5 nm.

Synthesis of SiO_2/Au/RF composites

The as-prepared SiO_2 spheres were transferred to a mixture of 2-propanol (20 mL) and APTES (50 uL) and heated to 80 °C for 3 h to functionalize the silica surface with $-NH_2$ groups.[21] Subsequently, the surface modified particles were washed with ethanol and dispersed in deionized water. The SiO_2/Au particles were prepared by mixing 60 ml of the Au solution with 270 mg of modified SiO_2 spheres under sonication. After that, the particles were centrifuged and redispersed in 60 ml of deionized water, mixed with an aqueous solution of CTAB (1 mL, 0.01 M) under vigorous stirring. After aging for 30 min, resorcinol (0.08 g), formaldehyde solution (0.12 mL) and ammonium hydroxide aqueous solution were added to the above suspension.[22]

Synthesis of Au/C thin sheets

The RF resin was first converted to carbon by heating the SiO_2/Au/RF composites at a high temperature (600, 700 and 800 °C) for 4 h under nitrogen atmosphere, respectively. After carbonization, the powders were etched in an aqueous solution containing 1 M NaOH under stirring at 50 °C for 24 h. The Au/C hollow spheres were collected by cleaning and drying the products. Finally, Au/C thin sheets were obtained by grinding the composite hollow spheres manually in a mortar.

Characterization

The sample morphology was characterized using a transmission electron microscope (TEM). The surface area of the samples was measured by the Brunauer–Emmett–Teller (BET) method using nitrogen adsorption and desorption isotherms on a high speed gas sorption analyzer (NOVA4000). A probe type Ocean Optics HR2000CG-UV-NIR spectrometer was used to measure the UV-vis spectra of the colloidal solutions to monitor the catalytic reduction of 4-nitrophenol and nitrobenzene as well as the optical property of the as-prepared Au solution.

Catalytic reduction of 4-nitrophenol and nitrobenzene

The reduction of 4-nitrophenol and nitrobenzene by $NaBH_4$ were chosen as model reactions to test the catalytic activity and stability of the Au/C catalysts. Aqueous solutions of 4-nitrophenol (0.15 mL, 0.001 M, or nitrobenzene) and $NaBH_4$ (1.0 mL, 0.20 M) were added to deionized water (1.5 mL) in a quartz cuvette. After injecting the catalyst particles (0.020 mL, 1 mg/ml), the bright yellow solution gradually faded as the reaction proceeded. UV-vis spectra were recorded in-situ at regular interval to monitor the progress of the reaction.

Results and Discussion

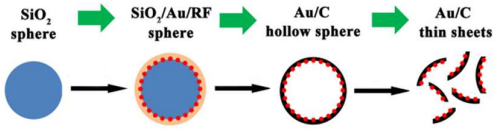

Scheme. 1 Illustration of the procedures for the synthesis of Au/C thin sheets.

The synthesis of the Au/C thin sheets combines simple sol-gel, calcination and selectively etching processes, as illustrated in Scheme. 1. Uniform SiO_2 templates with controllable diameters were first synthesized using the Stöber method,[19] and then functionalized with amine groups by reacting with APTES through surface siloxane linkage. Afterwards, ultrafine citrate-stabilized AuNPs (less than 5 nm in diameter) were loaded onto the surface of the SiO_2 spheres through the strong chemical affinity between Au and primary amines. As both the SiO_2/Au colloids and phenol groups were negatively charged in alkaline environment,[22] the SiO_2/Au colloids were modified by a cationic surfactant (CTAB) to reduce the negative surface charges to facilitate the formation of a uniform shell through base–catalyzed polymerization of resorcinol and formaldehyde. The RF resin was subsequently converted into carbon at high temperatures under an inert atmosphere, producing SiO_2/Au/C spheres. SiO_2 template was then etched by 1 M NaOH solution, yielding Au/C hollow spheres with AuNPs anchored on the inner wall of the carbon shells. Finally, the carbon shells were crushed by grinding to produce Au/C thin sheets.

Nanoscale

ARTICLE

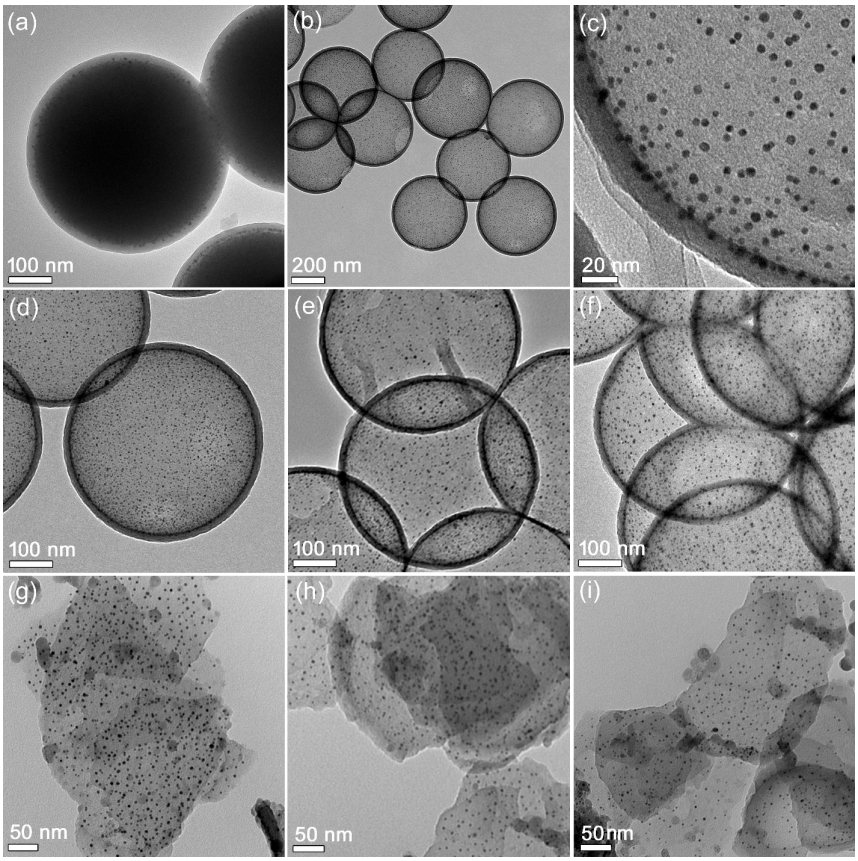

Fig. 1 TEM images of a) SiO_2/Au/RF spheres; b-f) Au/C hollow spheres produced by calcination at 600°C (b-d); 700 °C (e); and 800 °C (f), respectively; g-i) Au/C thin sheets produced by calcination at 600, 700 and 800 °C respectively.

Fig. 1a shows the representative TEM images of the SiO_2/Au/RF spheres. RF resin with a thickness of ~20 nm was evenly coated on the SiO_2 templates. A relatively high density ultrafine AuNPs could be found uniformly distributed at the interface between the core and shell. After carbonization and subsequent removal of the SiO_2 templates, hollow carbon spheres with numerous AuNPs decorated on their inner surfaces were obtained (Fig. 1b, c), with uniformity and spherical morphology well preserved. The shell shrank to ~15 nm after carbonization, enabling partial embedment of AuNPs into the carbon shells and enhancing their stability against de-attachment and sintering (Fig. 1c). Without such a tight contact, the AuNPs would easily detach from the support surface and fuse together especially during thermal treatment, as reported in the previous studies involving AuNPs and SiO_2 shells.[23,24] In our case, due to the partial embedment of AuNPs in the carbon shells, the dispersion and size of AuNPs could be well maintained even after high temperature treatments at 600, 700 and 800 °C (Fig. 1d-f). In order to expose the AuNPs to reactants during catalysis, the hollow composite spheres were crushed into thin sheets by manually grinding in a mortar for 10 minutes. As shown in Fig. 1g-i, the ultrafine AuNPs could still robustly anchor on the carbon sheets and remain uniformly distributed. No detached AuNPs were observed outside the carbon sheets.

A survey of particles in Fig. 1g indicates they have an average diameter of ~4.4 nm and size distribution in the range of 2.6 to 6.0 nm (Fig. S1a). The UV-vis absorption spectrum of the as-synthesized AuNP solution shows an absorption peak at ~511 nm (Fig. S1b), which is consistent with the small particle size observed by TEM imaging. These results suggest that the ultrafine AuNPs can preserve their sizes and dispersion even after the high temperature calcination, alkali etching, and mechanical grinding. The remarkable thermal and mechanical stability of AuNPs can be ascribed to the partial embedment of AuNPs into the carbon sheets, which benefits the catalytic stability and reusability of the materials as demonstrated later.

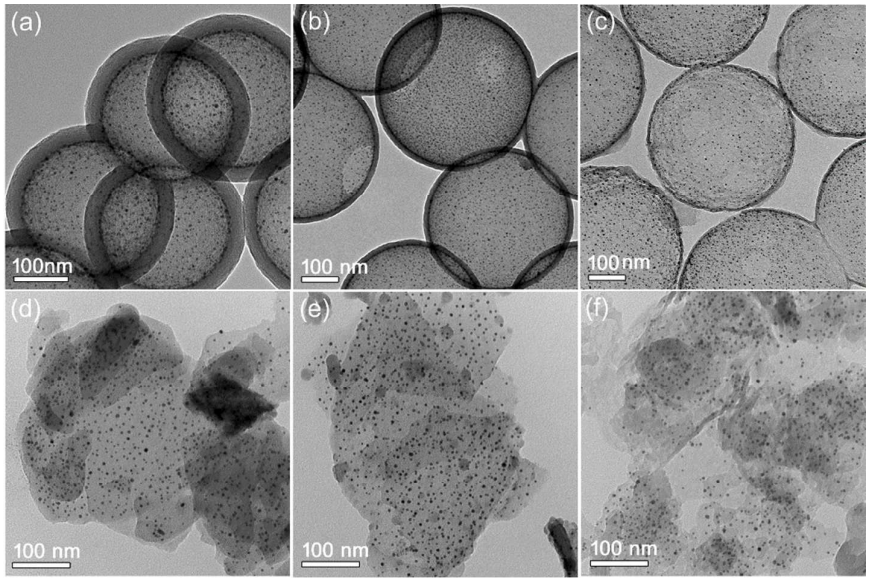

Fig. 2 TEM images of Au/C hollow spheres before and after being grinded into sheets. The original carbon shell thicknesses are: a, d) 32 nm, b, e) 15 nm, and c, f) 8 nm. The samples were prepared by calcination at 600 °C.

Table 1 Catalytic activity of Au/C hollow spheres and thin sheets in the reduction of 4-nitrophenol and nitrobenzene.

Samples	4-nitrophenol k (min^{-1}) Au/C hollow spheres	4-nitrophenol k (min^{-1}) Au/C thin sheets	Nitrobenzene k (min^{-1}) Au/C hollow spheres	Nitrobenzene k (min^{-1}) Au/C thin sheets
C600[a]	1.64	3.42	2.78	3.61
C700[b]	0.98	3.26	1.94	3.45
C800[c]	0.40	3.07	0.86	3.28
T8[d]	3.23	3.60	3.46	3.91
T15[e]	1.64	3.42	2.78	3.61
T32[f]	0.45	3.24	0.94	3.39

a, *b* and *c*: the number denotes the carbonization temperature. *d*, *e* and *f*: the number denotes the thickness of the carbon shells.

The thickness of carbon shell could be tuned by varying the concentration of RF precursors during synthesis. As displayed in Fig. 2, the thickness of the carbon shell was decreased from 32 to 8 nm by reducing the amount of resorcinol from 1.0 to 0.05 g with a fixed ratio of resorcinol to formaldehyde. It can also be seen that the distribution and particle size of AuNPs were not significantly affected by the thickness of the carbon layer.

The reduction of 4-nitrophenol and nitrobenzene in the presence of $NaBH_4$ were used as model reactions to evaluate the catalytic performance of the Au/C thin sheets.[25, 26] Fig. 3 shows the typical change of UV-vis absorption of the reaction mixture when catalyzed by the Au/C thin sheets prepared by calcination at 600 °C. The original aqueous 4-nitrophenol solution was yellow and showed characteristic absorption at the wavelength of 317 nm. Upon addition of $NaBH_4$ solution, the absorption peak shifted to 400 nm due to the formation of 4-nitrophenolate (Fig. 3a).[27] Before the addition of Au/C thin sheets, the peak intensity at 400 nm kept constant, suggesting no occurrence of reduction reaction (Inset of Fig. 3a). After adding Au/C catalysts into the solution, the absorption peak started to decrease, while a new peak at 300 nm characteristic of 4-aminophenol appeared accordingly. The reduction reaction completed within 150 s, which was evidenced by the disappearance of the characteristic peak at 400 nm as well as the yellow color of the solution (Fig. 3b). The ratios of C_t and C_0, which are the 4-nitrophenol concentrations at time t and 0 min, respectively, were determined by the relative absorption intensity at 400 nm (A_t /A_0). Since the amount of $NaBH_4$ is excessive, the catalytic reaction follows the pseudo first-order kinetics. The reaction rate constant k was calculated from the slope of the plots of $\ln(C_t/C_0)$ *vs*. time. The test of Au/C hollow spheres was conducted in the same way as Au/C thin sheets.

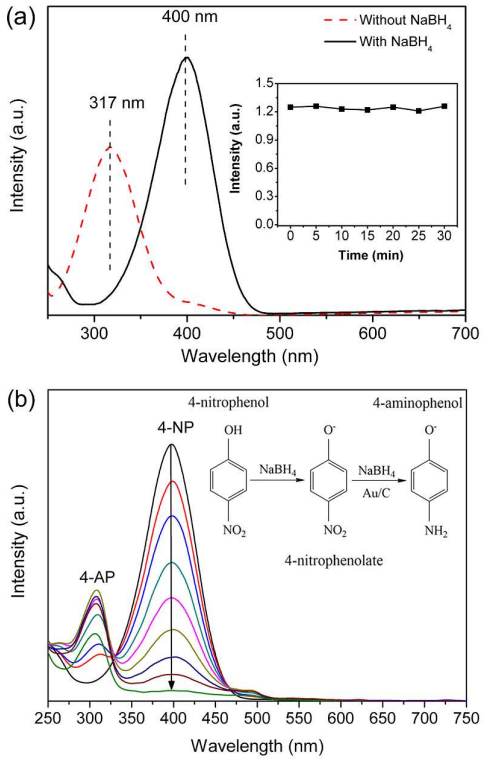

Fig. 3 a) UV-vis spectra of 4-nitrophenol solution with and without $NaBH_4$. The inset shows the variation in intensity of the peak at 400 nm when 4-nitrophenol was reacting with $NaBH_4$ in the absence of Au catalysts. b) Time-dependent UV-vis spectral change of the reduction of 4-nitrophenol catalyzed by Au/C thin sheets with carbon thickness of 15 nm prepared by calcination at 600 °C. The interval between each curve is 12 seconds. (4-NP and 4-AP denote 4-nitrophenol and 4-aminophenol, respectively.)

Fig. 4 compares the *k* values of the Au/C catalysts produced under different experimental conditions. As shown in Fig. 4a, the thickness of the carbon shell has a significant effect on the catalytic activities of the Au/C hollow spheres. Due to the reduced diffusion distance for the reactants, the rate constant *k* increased significantly from 0.45 to 3.23 min^{-1} as the shell thickness decreased from 32 to 8 nm. We believe the large increase in the reaction rates with the thinner shells is due to the enhanced mass diffusion associated with their shorter diffusion length and more porous nature. When the same hollow spheres were mechanically grinded into broken pieces (i.e. Au/C thin sheets) and then used as catalysts, the calculated *k* values varied accordingly from 3.24 to 3.60 min^{-1} (Fig. 4b). In this case, the thickness of the carbon shells did not show significant impact to the reaction rates because the Au NPs were exposed to the reaction directly now. It is apparent that material diffusion was hindered by thicker shells in the cases of hollow spheres, but the problem was relieved when the shells were cracked and all AuNPs were exposed to the reactants. We also notice that the *k* value of Au/C spheres (8 nm thick, Fig. 4a) was similar to the corresponding broken sheets (8 nm thick, Fig. 4b). In addition to their shorter diffusion length due to the smaller shell thickness, a considerable amount of pores have been created in the shells as proven below during carbonization so that reactants can access the AuNP surface as easily as the case when the shells are open.

The effect of calcination temperature was also investigated. The *k* constant decreases with the increase of carbonization temperature from 600 to 800 °C of the Au/C hollow spheres with shell thickness of 15 nm (Fig. 4c). Since the AuNPs size and distribution were not significantly affected by the heat treatment temperature as shown in Fig. 1, the big difference of the catalytic activity could be correlated to structure of the carbon shells. The N_2 adsorption–desorption isotherms were therefore used to study the surface area and porosity of the Au/C hollow spheres (Fig. S2). The isotherm shows type-IV curve and H2-type hysteresis loop, reflecting the mesoporous characteristic with "ink-bottle" type pores.[28] The pores were derived from the pyrolysis of the RF resin, which included the evaporation of the non-crosslinked species (including monomers, oligomers, and solvents in polymer networks) and the removal of H, O, C atoms from the polymer chains.[29] The BET surface areas of the samples calcined at 600, 700 and 800 °C were found to be 294.1, 230.4 and 132.2 m^2/g, respectively. The same dependence was also observed previously in Yoon's and Yu's studies, likely due to partial collapse of the pores and densification of the shells at higher temperatures.[30, 31] As generally expected, a larger surface area correlates to a higher porosity, which is beneficial to the diffusion of reactants from outside of carbon spheres to the surface of enclosed AuNPs. Therefore, the Au/C hollow spheres calcined at 600 °C exhibited the highest catalytic activity. The pore size distribution calculated by the BJH (Barrett–Joyner–Halender) method indicates the pores in the sample calcined at 600 °C were less than 5 nm (Inset of Fig. S2). After being broken into small pieces, again, the catalytic activity of formed Au/C shin sheets were much improved and the difference of the activity was also much reduced among the three samples.

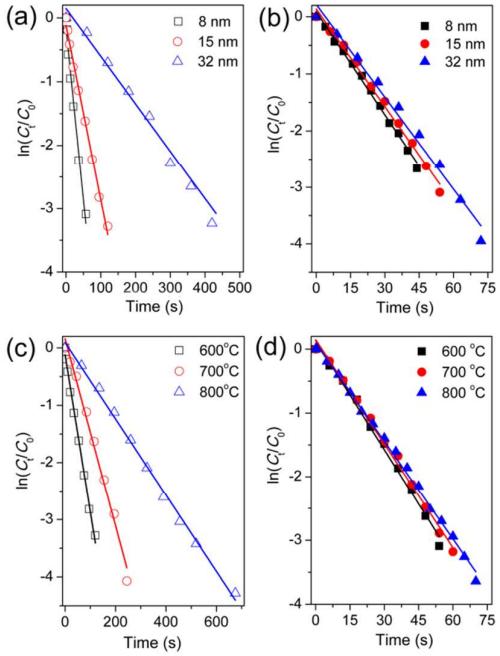

Fig. 4 Kinetic analysis of the catalytic reduction of 4-nitrophenol in the presence of various Au/C catalysts: a,b) Au/C hollow spheres (a) and Au/C thin sheets (b) (both prepared by calcination at 600 °C) with carbon thickness of 8, 15 and 32 nm; c,d) Au/C hollow spheres (c) and Au/C thin sheets (d) with carbon thickness of 15 nm prepared by carbonization at 600, 700 and 800 °C.

Besides the reduction of hydrophilic 4-nitrophenol, the Au/C catalysts also showed outstanding catalytic performance for the reduction of hydrophobic nitrobenzene (Fig. S3 and Fig. S4).[32] The kinetic rate constant *k* showed a similar tendency as 4-nitrophenol reduction and was also summarized in Table 1. We notice that the *k* values obtained for the reduction of nitrobenzene are higher than those of 4-nitrophenol, which implies that the carbon shell favors the enrichment of hydrophobic nitrobenzene. It is known that pristine carbon materials are hydrophobic. The templating synthesis however involves chemical etching by a strong base which produces hydroxyl and carboxylate groups on the carbon surface and renders water dispersity to the inherently hydrophobic carbon shells. Such a unique structure makes it possible to use the Au/C nanosheets for catalyzing the reactions of both hydrophilic and hydrophobic substrates.

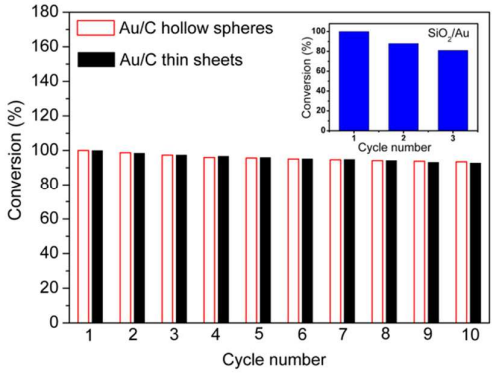

Fig. 5 Conversions of 4-nitrophenol in ten cycles catalyzed by Au/C hollow spheres and Au/C thin sheets (carbon thickness of 15 nm). The samples were prepared by calcination at 600 °C. Inset: Conversions of 4-nitrophenol in three cycles catalyzed by SiO_2/Au spheres.

Stability and reusability are important concerns for heterogeneous catalysts. The Au/C hollow spheres and thin sheets (600 °C, 15 nm thick) were therefore used in the reduction of 4-nitrophenol over ten times. In general, the yolk-shell structured catalysts exhibited high stabilities in recycling measurements due to the protection of the outer shells.[23, 33] Likewise, the Au/C hollow spheres showed no severe decay in catalytic activities in repeated experiments, as shown in Fig. 5. More importantly, after being grinded into smaller pieces with Au surface exposed, the Au/C thin sheets preserved the excellent stability and reusability, and were still quite active with the conversion efficiency close to 93% after ten cycles of reactions. The TEM image of Au/C thin sheets after the cycling test showed no detachment of Au NPs from or their agglomeration on carbon sheets (Fig. S5). Furthermore, the effect of heat treatment temperature was also checked by measuring the cycling property of Au/C sheets treated at an even higher temperature of 800 °C (15 nm in thickness). The stability was found to be similar to the catalyst heated at 600 °C (Fig. S6). The slight decrease in catalytic efficiencies may be ascribed to the minor loss of catalysts during recycling, and the passivation of the AuNPs by 4-aminophenol.[34] For a comparison, the reduction reaction with SiO_2/Au particles, where AuNPs were only simply adsorbed on large SiO_2 particles, were carried out under the same conditions. Due to weak anchoring on AuNPs, the catalytic rate decayed fast in only three cycles (Inset in Fig. 5). Such poor stability can be ascribed to the detachment of tiny AuNPs from the surface of SiO_2 particle during recycling. The excellent catalytic stability of Au/C hollow spheres and thin sheets suggests that the AuNPs are strongly attached to the surface of the carbon layer. We believe such strong anchoring benefits from the partial embedment of the particles into the shell, although direct imaging of such morphological relation is challenging with conventional microscopy analytic tools.

Conclusions

We proposed a new and unique strategy to stabilize ultrafine Au nanoparticles on thin carbon sheets. With densely distributed AuNPs, the Au/C thin sheets exhibit high stability and excellent catalytic activity for reduction reactions of both hydrophilic 4-nitrophenol and hydrophobic nitrobenzene. The superior stability of the Au/C shells or thin sheets derives from the structural advantage of the composite in that the partial embedment of AuNPs into the surface of the carbon shells leads to a strong anchoring of AuNPs to the support. The shrinkage of the resin shells during calcination facilitates the strong anchoring of the AuNPs, resulting in composite catalysts that could sustain high temperature or mechanical post-treatments. Meanwhile, diffusion of reactants to the surface of AuNPs could be maximized by reducing the thickness of the hollow shells or simply by cracking the shells into thin carbon sheets, both significantly benefiting the high catalytic efficiency. The excellent catalytic properties for both hydrophilic and hydrophobic reactants endow the novel Au/C thin sheets broad applications. It is believed that this synthesis method can be easily extended to the fabrication of other highly efficient and stable heterogeneous catalysts.

Acknowledgements

This work was partly supported by the U.S. Department of Energy, Office of Science, Basic Energy Sciences, Chemical Sciences, Geosciences, & Biosciences (CSGB) Division, under Award No. DE-SC0002247. Liu was supported by the National Natural Science Foundation of China (No. 51102006) Beijing Municipal Science and Technology Project (No.D14110300240000). Yin is a member of the Center for Catalysis at the University of California, Riverside (more details can be found at catalysis.ucr.edu).

Notes and references

1. X. Y. Li, X. Wang, S. Y. Song, D. P. Liu and H. J. Zhang, *Chemistry-a European Journal*, 2012, **18**, 7601-7607.
2. S. Wang, Q. Zhao, H. Wei, J.-Q. Wang, M. Cho, H. S. Cho, O. Terasaki and Y. Wan, *Journal Of the American Chemical Society*, 2013, **135**, 11849-11860.
3. S. W. Kim, M. Kim, W. Y. Lee and T. Hyeon, *Journal Of the American Chemical Society*, 2002, **124**, 7642-7643.
4. K. Na, K. M. Choi, O. M. Yaghi and G. A. Somorjai, *Nano Letters*, 2014, **14**, 5979-5983.
5. A. Dhakshinamoorthy and H. Garcia, *Chemical Society Reviews*, 2012, **41**, 5262-5284.
6. F. Zaera, *Chemical Society Reviews*, 2013, **42**, 2746-2762.
7. C. Ma, W. Xue, J. Li, W. Xing and Z. Hao, *Green Chemistry*, 2013, **15**, 1035-1041.
8. T. T. Zhang, H. Y. Zhao, S. N. He, K. Liu, H. Y. Liu, Y. D. Yin and C. B. Gao, *Acs Nano*, 2014, **8**, 7297-7304.
9. R. Guttel, M. Paul and F. Schuth, *Chemical Communications*, 2010, **46**, 895-897.
10. I. Lee, J. B. Joo, Y. D. Yin and F. Zaera, *Angewandte Chemie-International Edition*, 2011, **50**, 10208-10211.
11. J. Han, Y. Liu and R. Guo, *Advanced Functional Materials*, 2009, **19**, 1112-1117.

12. H. B. Chong, P. Li, J. Xiang, F. Y. Fu, D. D. Zhang, X. R. Ran and M. Z. Zhu, *Nanoscale*, 2013, **5**, 7622-7628.
13. Y. D. Yin, R. M. Rioux, C. K. Erdonmez, S. Hughes, G. A. Somorjai and A. P. Alivisatos, *Science*, 2004, **304**, 711-714.
14. J. Ge, Q. Zhang, T. Zhang and Y. Yin, *Angewandte Chemie-International Edition*, 2008, **47**, 8924-8928.
15. H. A. Gasteiger, S. S. Kocha, B. Sompalli and F. T. Wagner, *Appl. Catal., B*, 2005, **56**, 9-35.
16. J. B. Yoo, H. J. Yoo, B. W. Lim, K. H. Lee, M. H. Kim, D. Kang and N. H. Hur, *Chemsuschem*, 2012, **5**, 2334-2340.
17. T. Zeng, X. L. Zhang, S. H. Wang, Y. R. Ma, H. Y. Niu and Y. Q. Cai, *J. Mater. Chem. A*, 2013, **1**, 11641-11647.
18. B. Liu, W. Zhang, H. L. Feng and X. L. Yang, *Chemical Communications*, 2011, **47**, 11727-11729.
19. Q. Zhang, D. Q. Lima, I. Lee, F. Zaera, M. F. Chi and Y. D. Yin, *Angewandte Chemie-International Edition*, 2011, **50**, 7088-7092.
20. W. Stober, A. Fink and B. E., *Journal of Colloid and Interface Science* 1969, **26**, 62-69.
21. Q. Zhang, J. P. Ge, J. Goebl, Y. X. Hu, Y. G. Sun and Y. D. Yin, *Advanced Materials*, 2010, **22**, 1905-1909.
22. N. Li, Q. Zhang, J. Liu, J. Joo, A. Lee, Y. Gan and Y. D. Yin, *Chemical Communications*, 2013, **49**, 5135-5137.
23. Y. Yin, M. Chen, S. Zhou and L. Wu, *Journal Of Materials Chemistry*, 2012, **22**, 11245-11251.
24. X. W. Lou, C. Yuan, E. Rhoades, Q. Zhang and L. A. Archer, *Advanced Functional Materials*, 2006, **16**, 1679-1684.
25. J. Lee, J. C. Park and H. Song, *Advanced Materials*, 2008, **20**, 1523-1528.
26. C. H. Yuan, W. A. Luo, L. N. Zhong, H. J. Deng, J. Liu, Y. T. Xu and L. Z. Dai, *Angewandte Chemie-International Edition*, 2011, **50**, 3515-3519.
27. N. Pradhan, A. Pal and T. Pal, *Langmuir*, 2001, **17**, 1800-1802.
28. G. Liu, Y. Liu, Z. L. Wang, X. Z. Liao, S. J. Wu, W. X. Zhang and M. J. Jia, *Microporous and Mesoporous Materials*, 2008, **116**, 439-444.
29. H. X. Yu, Q. Zhang, J. B. Joo, N. Li, G. D. Moon, S. Y. Tao, L. J. Wang and Y. D. Yin, *J. Mater. Chem. A*, 2013, **1**, 12198-12205.
30. S. Yoon, S. M. Oh and C. Lee, *Materials Research Bulletin*, 2009, **44**, 1663-1669.
31. H. X. Yu, Q. Zhang, J. B. Joo, N. Li, G. D. Moon, S. Y. Tao, L. J. Wang and Y. D. Yin, *Journal of Materials Chemistry A*, 2013, **1**, 12198-12205.
32. B. Y. Guan, X. Wang, Y. Xiao, Y. L. Liu and Q. S. Huo, *Nanoscale*, 2013, **5**, 2469-2475.
33. Y. Yu, C. Y. Cao, Z. Chen, H. Liu, P. Li, Z. F. Dou and W. G. Song, *Chemical Communications*, 2013, **49**, 3116-3118.
34. F.-h. Lin and R.-a. Doong, *Journal of Physical Chemistry C*, 2011, **115**, 6591-6598.

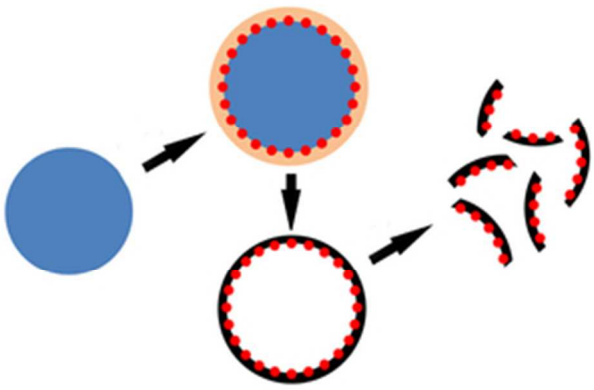

Graphic abstract
27x18mm (300 x 300 DPI)